ON THE STABILITY OF PRESSURE AND VELOCITY COMPUTATIONS FOR HETEROGENEOUS RESERVOIRS

ARE MAGNUS BRUASET* AND BJØRN FREDRIK NIELSEN**

Abstract. This paper is concerned with the stability of self-adjoint second order elliptic problems with respect to perturbations of the involved coefficient functions. In particular, we study such behaviour for the pressure equation related to incompressible or steady state flow in a heterogeneous reservoir. We establish analytical estimates on the changes in the pressure and velocity caused by mobility perturbations measured by the L^∞ norm. This stability analysis is complemented by numerical experiments.

Key words. reservoir simulation, elliptic problems, stability analysis, perturbation theory

AMS(MOS) subject classifications. 35B30, 35J25, 65J10.

1. Introduction. In reservoir simulation, collected data on geology is the backbone of massive computations that are used for prediction and optimization of hydrocarbon production. As for most types of simulation, there are many possibilities for introducing nonphysical effects or even errors that can turn any computation into nonsense. Typically, such divergence from the underlying process could be caused by the use of incompetent physical or mathematical models, unsuitable numerical methods or erroneous computer codes. Even when accepting the chosen model and its implementation, the simulation may be badly influenced by noisy input data or inaccuracies in the interpretation of physical measurements. For this reason, it is important to know how the solution of established mathematical models are affected by variations in the input data, e.g. in material coefficients and boundary conditions. The traditional stability analysis of elliptic problems seems to pay less attention to perturbations of the coefficient functions than to perturbations of the boundary conditions and source terms. As far as material coefficients are concerned, most results deal with regularity assumptions, see Dautray and Lions [4, Ch. VII] and Hackbusch [12, Ch. 9]. However, this paper will investigate the property of stability with respect to perturbations of the involved coefficients. In particular, we study the pressure and velocity in a heterogeneous reservoir subject to variations in certain geological parameters.

It is generally accepted that mathematical models of fluid flow in porous media may be stated in terms of coupled partial differential equations, see for instance Ewing [7] or Peaceman [15]. In this

* SINTEF Applied Mathematics, P.O. Box 124 Blindern, N-0314 Oslo, Norway.

Email: Are.Magnus.Bruaset@si.sintef.no. This author's work has been supported by The Research Council of Norway under grant no. 412.93/005 and through the strategic technology program STP 28402: *Toolkits in Industrial Mathematics* at SINTEF.

** Department of Informatics, University of Oslo, P.O. Box 1080 Blindern, N-0316 Oslo, Norway.

Email: bjornn@ifi.uio.no.. This author's work has been supported by The Research Council of Norway (NFR) under grant no. 107643/431.

paper we will concentrate on the elliptic equation

$$\nabla \cdot [\Lambda (\nabla p - \rho g \nabla D)] + \frac{q}{\rho} = 0 \quad \text{in } \Omega \subset \mathbb{R}^2, \tag{1.1}$$

where the unknown fluid pressure p is related to incompressible or steady-state flow. Moreover, the function D denotes the depth of the reservoir measured in the direction of gravity, while g is the gravitational constant and ρ is the fluid density. Throughout this paper we will assume that ρ, g and ∇D are constant over Ω. The second order mobility tensor Λ incorporates physical parameters such as the permeability of the medium and the viscosity of the fluid. Depending on the exact definition of Λ, (1.1) may be taken as a prototype of the pressure equations for single-phase as well as multi-phase flows. For heterogeneous reservoirs, the mobility may have large variations and even discontinuities. Typically, Λ can be piecewise constant, thus representing the effect of different reservoir layers. The function q in (1.1) represents internal sources. Typically, q will be a combination of Dirac delta functions that implement injection and production wells located inside Ω.

The boundary $\partial\Omega$, which is assumed to be sufficiently smooth, can be divided into three disjoint segments Γ_{in}, Γ_{out} and Γ_{else}. The pressure equation (1.1) is then subject to the boundary conditions

$$\begin{aligned} \mathbf{v} \cdot \mathbf{n} &= g_{\text{in}} && \text{on } \Gamma_{\text{in}}, \\ p &= p_{\text{out}} && \text{on } \Gamma_{\text{out}}, \\ \mathbf{v} \cdot \mathbf{n} &= 0 && \text{on } \Gamma_{\text{else}}. \end{aligned} \tag{1.2}$$

Here $\mathbf{n}$ denotes the outwards directed normal vector of unit length, while the Darcy velocity $\mathbf{v}$ is defined as

$$\mathbf{v} = -\Lambda (\nabla p - \rho g \nabla D) . \tag{1.3}$$

In a reservoir setting, the boundary segments Γ_{in} and Γ_{out} refer to inwards and outwards fluxes, respectively. The remaining part of the boundary, Γ_{else}, is subject to no-flux conditions.

The remainder of this paper is organized as follows: In the next section we study perturbations of the coefficient functions for an operator equation having the form of the pressure equation. This leads to an abstract error estimate which we apply to our model problem in §3. The main result of this paper shows that the pressure and the velocity field of the pressure equation depends Lipschitz continuously on perturbations in the mobility tensor measured in the L^∞ norm. In §4 we complement the stability analysis through a series of numerical experiments based on conforming as well as mixed finite element procedures. Finally, we summarize the results in §5.

2. Stability analysis in an abstract Hilbert space setting. Instead of studying perturbations in the mobility tensor Λ for the pressure equation (1.1) directly, we will first consider this type of problem for more general operator equations. Then, in the next section, the theory is applied to our model problem (1.1)-(1.2). It should be noted that a perturbation in the mobility tensor Λ causes

changes in the bilinear form and the functionals associated with the weak formulation of the problem (1.1)-(1.2). With this in mind, we proceed as follows:

Let $\mathcal{H}$ be a real Hilbert space with inner-product $(\cdot,\cdot)$ and norm $\|\cdot\|$. Consider the following two linear variational problems: Find $u_i \in \mathcal{H}$ such that

$$a_i(u_i,\psi) + b_i(\psi) = f(\psi) \quad \text{for all } \psi \in \mathcal{H}, \text{ and for } i = 1,2. \tag{2.1}$$

Assume that $f(\cdot)$ and $b_i(\cdot)$ for $i = 1,2$ are bounded linear functionals on $\mathcal{H}$, and that $a_i(\cdot,\cdot)$ for $i = 1,2$ are bilinear, continuous and $\mathcal{H}$-elliptic forms on $\mathcal{H} \times \mathcal{H}$. That is, there exists constants L, N, k and K such that

$$\begin{aligned} &|f(\psi)| \le L \,\|\psi\| && \text{for all } \psi \in \mathcal{H} \\ &|b_i(\psi)| \le N \,\|\psi\| && \text{for all } \psi \in \mathcal{H} \\ &a_i(\psi,\psi) \ge k \,\|\psi\|^2 && \text{for all } \psi \in \mathcal{H} \\ &|a_i(u,\psi)| \le K \,\|u\|\,\|\psi\| && \text{for all } u,\psi \in \mathcal{H} \end{aligned} \tag{2.2}$$

Notice that we assume the existence of a common bound N for $b_i(\cdot)$ and common bounds k and K for $a_i(\cdot,\cdot)$, $i = 1,2$.

It follows from the Lax-Milgram theorem (see for instance Dautray and Lions [4] or Gilbarg and Trudinger [11]) that the problem (2.1) has a unique solution $u_i \in \mathcal{H}$ for $i = 1,2$. Moreover, by choosing $\psi = u_i$ in (2.1) and applying (2.2) we get the following a priori bound

$$\|u_i\| \le \frac{L+N}{k}, \quad \text{for } i = 1,2. \tag{2.3}$$

Next, assume that the bilinear forms and the linear functionals are close in the sense that there exist positive numbers A and B such that

$$|a_2(u,\psi) - a_1(u,\psi)| \le A\,\|u\|\,\|\psi\| \quad \text{and} \quad |b_2(\psi) - b_1(\psi)| \le B\,\|\psi\|, \tag{2.4}$$

for all $u, \psi \in \mathcal{H}$. Now, the question is: how close are the two solutions of the problems in (2.1)?

THEOREM 2.1. *Let u_1 and u_2 be the respective solutions of (2.1). If the assumptions (2.2) and (2.4) hold, then*

$$\|u_2 - u_1\| \le \left(\frac{L+N}{k^2}\right) A + \frac{B}{k}. \tag{2.5}$$

Proof. Subtracting (2.1) with $i = 1$ from (2.1) with $i = 2$ we get

$$a_2(u_2,\psi) - a_1(u_1,\psi) + b_2(\psi) - b_1(\psi) = 0.$$

Which is equivalent to

$$a_2(u_2,\psi) - a_2(u_1,\psi) + a_2(u_1,\psi) - a_1(u_1,\psi) + b_2(\psi) - b_1(\psi) = 0.$$

Since $u_1, u_2 \in \mathcal{H}$ we may choose $\psi = u_2 - u_1$ to obtain

$$a_2(u_2-u_1, u_2-u_1) = -a_2(u_1, u_2-u_1) + a_1(u_1, u_2-u_1) - b_2(u_2-u_1) + b_1(u_2-u_1),$$

where we have used the fact that $a_2(\cdot,\cdot)$ is a bilinear form. Applying (2.2) and the triangle inequality we get

$$k \,\|u_2-u_1\|^2 \leq |a_2(u_1, u_2-u_1) - a_1(u_1, u_2-u_1)| + |b_2(u_2-u_1) - b_1(u_2-u_1)|. \tag{2.6}$$

By (2.4) and (2.3) it is easy to see that

$$|a_2(u_1, u_2-u_1) - a_1(u_1, u_2-u_1)| \leq A \,\|u_1\| \,\|u_2-u_1\| \leq \left(\frac{L+N}{k}\right) A \,\|u_2-u_1\|.$$

Finally, combining this inequality with (2.6) and (2.4) gives

$$k \,\|u_2-u_1\|^2 \leq \left(\frac{L+N}{k}\right) A \,\|u_2-u_1\| + B \,\|u_2-u_1\|,$$

which finishes the proof. □

3. Stability analysis of the pressure equation. In this section we will study perturbations of the mobility tensor Λ, measured by the L^∞ norm. In particular, we will show that the pressure p and the velocity $\mathbf{v}$ for the problem (1.1)-(1.2) depend continuously on Λ. Before presenting the main result in this paper, we introduce some notation and an appropriate weak formulation of our model problem.

In this paper we use $L^p(Y)$, for $Y = \Omega, \Gamma_{\text{in}}$, to denote the classical L^p spaces of real valued functions defined on Y. On $L^2(\Omega) \times L^2(\Omega)$ we introduce the norm $\|\cdot\|_{(L^2(\Omega))^2}$ given by

$$\|\mathbf{w}\|^2_{(L^2(\Omega))^2} = \|w_1\|^2_{L^2(\Omega)} + \|w_2\|^2_{L^2(\Omega)}$$

for $\mathbf{w} = (w_1, w_2)^T \in L^2(\Omega) \times L^2(\Omega)$. For $\mathbf{z} \in \mathbb{R}^2$, $|\mathbf{z}|$ denotes the Euclidean norm of $\mathbf{z}$. The Sobolev space $H^1(\Omega)$ is as usual defined by

$$H^1(\Omega) = \left\{ \psi \in L^2(\Omega);\ \frac{\partial \psi}{\partial x}, \frac{\partial \psi}{\partial y} \in L^2(\Omega) \right\},$$

where $\partial\psi/\partial x$ and $\partial\psi/\partial y$ are the distributional partial derivatives of ψ. The appropriate subspace for our model problem, due to the boundary conditions (1.2), is

$$V = \left\{ \psi \in H^1(\Omega);\ \psi = 0 \text{ on } \Gamma_{\text{out}} \right\}.$$

Now, the weak formulation of (1.1)-(1.2) can be defined as follows: Find $p \in H^1(\Omega)$ such that $p = p_{\text{out}}$ on Γ_{out} and

$$\int_\Omega \nabla\psi \cdot (\Lambda \nabla p)\, dx = \int_\Omega \frac{q}{\rho}\psi \, dx + \int_\Omega \nabla\psi \cdot (\rho g \Lambda \nabla D)\, dx - \int_{\Gamma_{\text{in}}} \psi g_{\text{in}} \, ds \tag{3.1}$$

for all $\psi \in V$. To get a well-posed variational problem (3.1), we will assume that

$$q \in L^2(\Omega), \quad D \in H^1(\Omega), \quad g_{\text{in}} \in L^2(\Gamma_{\text{in}}), \quad p_{\text{out}} \in H^{1/2}(\Gamma_{\text{out}}). \tag{3.2}$$

Moreover, recall that ρ, g and ∇D are constant over Ω.

In the weak formulation (3.1) the unknown function p is not in the same space as the variational function ψ. Therefore, in order to apply Theorem 2.1, it is convenient to introduce the following alternative formulation of this problem: Find $u \in V$ such that

$$\int_\Omega \nabla\psi \cdot (\Lambda \nabla u)\, dx + \int_\Omega \nabla\psi \cdot (\Lambda \nabla \overline{p}_{\text{out}})\, dx - \int_\Omega \nabla\psi \cdot (\rho g \Lambda \nabla D)\, dx = \int_\Omega \frac{q}{\rho}\psi\, dx - \int_{\Gamma_{\text{in}}} \psi g_{\text{in}}\, ds \tag{3.3}$$

for all $\psi \in V$. Here, $\overline{p}_{\text{out}} \in H^1(\Omega)$ denotes an extension of p_{out} to Ω. The existence of this extension follows from assumption (3.2) and the trace theorem. Moreover, it satisfies $T(\overline{p}_{\text{out}})|_{\Gamma_{\text{out}}} = p_{\text{out}}$, where $T : H^1(\Omega) \to H^{1/2}(\partial\Omega)$ denotes the trace operator. It is clear that if u is a solution of (3.3) then $p = u + \overline{p}_{\text{out}}$ is a solution of (3.1) and vice versa.

The main objective of this paper is to study perturbations of the mobility tensor, i.e., to find out whether the pressure p and the velocity $\mathbf{v}$ are stable with respect to perturbations of Λ. In order to define an appropriate set of mobility tensors, we consider the family of mappings

$$S = \left\{ \Lambda : \Omega \to \mathbb{R}^{2\times 2};\ \Lambda = \begin{pmatrix} \lambda & \gamma \\ \gamma & \eta \end{pmatrix} \text{ where } \lambda, \gamma, \eta \in L^\infty(\Omega) \right\}.$$

We will consider uniformly positive definite matrices. More precisely, for given real numbers $M \geq m > 0$, a collection $A_{m,M}$ of mobility tensors is defined by

$$A_{m,M} = \left\{ \Lambda \in S;\ m \leq \frac{\mathbf{z}^T \Lambda(\mathbf{x}) \mathbf{z}}{|\mathbf{z}|^2} \leq M \text{ for all } \mathbf{z} \in \mathbb{R}^2 \setminus \{0\} \text{ and } \mathbf{x} \in \Omega \right\}.$$

Notice that if $\Lambda \in A_{m,M}$ then $\Lambda(\mathbf{x})$ is positive definite throughout Ω, and the variational problem (3.1) is strictly elliptic, see for instance Dautray and Lions [5, Ch. II.8]. For $\Lambda \in A_{m,M}$ and $\mathbf{x} \in \Omega$ the operator norm $|\Lambda(\mathbf{x})|$ is, as usual, defined by

$$|\Lambda(\mathbf{x})| = \sup_{\mathbf{z} \in \mathbb{R}^2 \setminus \{0\}} \frac{|\Lambda(\mathbf{x})\mathbf{z}|}{|\mathbf{z}|}.$$

From the definition of $A_{m,M}$ it is easy to see that every mobility tensor $\Lambda \in A_{m,M}$ satisfies the inequality

$$m \leq |\Lambda(\mathbf{x})| \leq M \quad \text{for all } \mathbf{x} \in \Omega. \tag{3.4}$$

It follows from the Lax-Milgram theorem that if q, D, g_{in} and p_{out} satisfy (3.2) then the problem (3.1) has a unique solution $p \in H^1(\Omega)$ for every $\Lambda \in A_{m,M}$. Thus, we can study perturbations of the mobility tensor Λ such that the perturbated mobility tensor also belongs to $A_{m,M}$. Now, introduce

the notation

$$a(\Lambda; u, \psi) = \int_\Omega \nabla\psi \cdot (\Lambda \nabla u)\, dx$$
$$b(\Lambda; \psi) = \int_\Omega \nabla\psi \cdot (\Lambda \nabla \overline{p}_{\text{out}})\, dx - \int_\Omega \nabla\psi \cdot (\rho g \Lambda \nabla D)\, dx$$
$$f(\psi) = \int_\Omega \frac{q}{\rho}\psi\, dx - \int_{\Gamma_{\text{in}}} \psi g_{\text{in}}\, ds.$$

For every pair $\Lambda^{(1)}, \Lambda^{(2)} \in A_{m,M}$ of mobility tensors we get two problems of the form (3.3): Find $u_i \in V$ such that

$$a(\Lambda^{(i)}; u_i, \psi) + b(\Lambda^{(i)}, \psi) = f(\psi) \tag{3.5}$$

for all $\psi \in V$, and for $i = 1, 2$. As a consequence of Theorem 2.1, we obtain the following bound in terms of the L^∞ norm

$$\|\Lambda^{(1)} - \Lambda^{(2)}\|_{L^\infty(\Omega)} = \operatorname*{ess\,sup}_{x\in\Omega} |\Lambda^{(1)}(x) - \Lambda^{(2)}(x)|.$$

COROLLARY 3.1. *Let u_1 and u_2 denote the respective solutions of (3.5) associated with $\Lambda^{(1)}, \Lambda^{(2)} \in A_{m,M}$. Then $p_1 = u_1 + \overline{p}_{\text{out}}$ and $p_2 = u_2 + \overline{p}_{\text{out}}$ are the solutions of (3.1) corresponding to $\Lambda = \Lambda^{(1)}$ and $\Lambda = \Lambda^{(2)}$, respectively. Moreover, there exist constants $c_1, c_2 \in \mathbb{R}_+$ such that*

$$\|p_1 - p_2\|_{H^1(\Omega)} \le c_1 \|\Lambda^{(1)} - \Lambda^{(2)}\|_{L^\infty(\Omega)}$$

and

$$\|\mathbf{v}_1 - \mathbf{v}_2\|_{(L^2(\Omega))^2} \le c_2 \|\Lambda^{(1)} - \Lambda^{(2)}\|_{L^\infty(\Omega)},$$

where $\mathbf{v}_i = -\Lambda^{(i)}(\nabla p_i - \rho g \nabla D)$ for $i = 1, 2$.

Proof. Referring to the symbols used in §2 we put $\mathcal{H} = V$, $(\cdot,\cdot) = (\cdot,\cdot)_{H^1(\Omega)}$, $\|\cdot\| = \|\cdot\|_{H^1(\Omega)}$, $a_i(\cdot,\cdot) = a(\Lambda^{(i)};\cdot,\cdot)$ and $b_i(\cdot) = b(\Lambda^{(i)};\cdot)$, while $f(\cdot)$ is as defined above. Then it is easy to verify that (2.2) is satisfied with $N = M\|\overline{p}_{\text{out}}\|_{H^1(\Omega)} + M\|\rho g \nabla D\|_{(L^2(\Omega))^2}$, $L = \|q/\rho\|_{L^2(\Omega)} + \|T\|\,\|g_{\text{in}}\|_{L^2(\Gamma_{\text{in}})}$, $k = m/(1+P^2)$ and $K = M$. Here, $\|T\|$ denotes the operator norm of the trace operator, and P is the constant in Poincaré's inequality;

$$\|\psi\|_{L^2(\Omega)} \le P\left(\int_\Omega |\nabla\psi|^2\right)^{1/2} \quad \text{for all } \psi \in V,$$

see for instance Dautray and Lions [4, Ch. IV.7]. Moreover, (2.4) holds with $A = \|\Lambda^{(1)} - \Lambda^{(2)}\|_\infty$ and $B = (N/M)\|\Lambda^{(1)} - \Lambda^{(2)}\|_\infty$. Hence, from Theorem 2.1 we get

$$\|p_2 - p_1\|_{H^1(\Omega)} = \|u_2 + \overline{p}_{\text{out}} - (u_1 + \overline{p}_{\text{out}})\|_{H^1(\Omega)} \le \frac{L+N}{k^2}\|\Lambda^{(1)} - \Lambda^{(2)}\|_\infty + \frac{N}{kM}\|\Lambda^{(1)} - \Lambda^{(2)}\|_\infty.$$

Combining this inequality with the triangle inequality, the Hölder inequality and inequalities (3.4) and (2.3) it follows that

$$
\begin{aligned}
&\| \mathbf{v}_1 - \mathbf{v}_2 \|_{(L^2(\Omega))^2} = \| -\Lambda^{(1)}(\nabla p_1 - \rho g \nabla D) + \Lambda^{(2)}(\nabla p_2 - \rho g \nabla D) \|_{(L^2(\Omega))^2} \\
&= \| -\Lambda^{(1)}(\nabla p_1 - \rho g \nabla D) + \Lambda^{(2)}(\nabla p_2 - \rho g \nabla D) + \Lambda^{(1)} \nabla p_2 - \Lambda^{(1)} \nabla p_2 \|_{(L^2(\Omega))^2} \\
&\leq \| \Lambda^{(1)}(\nabla p_2 - \nabla p_1) \|_{(L^2(\Omega))^2} + \| (\Lambda^{(1)} - \Lambda^{(2)}) \rho g \nabla D \|_{(L^2(\Omega))^2} + \| (\Lambda^{(2)} - \Lambda^{(1)}) \nabla p_2 \|_{(L^2(\Omega))^2} \\
&\leq \| \Lambda^{(1)} \|_{L^\infty(\Omega)} \| p_1 - p_2 \|_{H^1(\Omega)} + \| \Lambda^{(1)} - \Lambda^{(2)} \|_{L^\infty(\Omega)} \| \rho g \nabla D \|_{(L^2(\Omega))^2} + \| \Lambda^{(1)} - \Lambda^{(2)} \|_{L^\infty(\Omega)} \| p_2 \|_{H^1(\Omega)} \\
&\leq M c_1 \| \Lambda^{(1)} - \Lambda^{(2)} \|_{L^\infty(\Omega)} + \| \rho g \nabla D \|_{(L^2(\Omega))^2} \| \Lambda^{(1)} - \Lambda^{(2)} \|_{L^\infty(\Omega)} \\
&\quad + \left(\frac{L+N}{k} + \| \overline{p}_{\text{out}} \|_{H^1(\Omega)} \right) \| \Lambda^{(1)} - \Lambda^{(2)} \|_{L^\infty(\Omega)},
\end{aligned}
$$

which completes the proof. □

Thus, we have shown that the pressure p and the velocity $\mathbf{v}$ are Lipschitz continuous with respect to perturbations of the mobility tensor, measured by the L^∞ norm.

4. Numerical experiments. In this section we present numerical results for two different cases covered by the stability analysis in §3. The first example illustrates the results of Corollary 3.1, while the next case shows that certain problems may be less sensitive to mobility perturbations than what is predicted by the estimates presented in §3. When presenting these experiments we solve the given problems for a sequence of mobility tensors $\{\Lambda_n^{(2)}\}_{n=0,1,\ldots}$. The corresponding pressure and velocity solutions $p_{2,n}$ and $\mathbf{v}_{2,n}$ are compared to the solutions p_1 and $\mathbf{v}_1$ obtained for the fixed mobility tensor $\Lambda^{(1)}$.

Throughout this section we let $q \equiv 0$, i.e., there are no internal sources. Thus, we implement injection and production in terms of the boundary conditions on Γ_{in} and Γ_{out}. In the context of reservoir simulation, this situation corresponds to Ω being a vertical section that is placed between two wells.

Based on the weak formulation (3.1), it is straight forward to define a conforming finite element method for the pressure equation (1.1). The experiments reported below have been carried out for bilinear shape functions on quadrilateral elements, where the values of p corresponding to the four vertices of each element represent the degrees of freedom. The resulting linear system of equations has been solved by the conjugate gradient (CG method combined with the ILU(0) preconditioner, see Meijerink and van der Vorst [14]. We have then used the zero vector as initial guess and halted the iterations as soon as $|\mathbf{b} - \mathbf{A}\mathbf{x}^k| \leq 10^{-8}$, where $\mathbf{x}^k$ denotes the kth CG iterate.

Independent of the experiments presented in §4.1 and §4.2, we have also solved the two model problems with a mixed finite element procedure. As will be discussed at the end of this section, the two alternative solution procedures lead to the same conclusions.

Using a superelement technique to construct the grid, the discontinuous behaviour of the mobility tensor can be represented independently of the global mesh parameter h. That is, we define a coarse

grid that has grid lines along the interfaces of any two adjacent layers in the reservoir Ω. We also ensure that grid lines are inserted to represent the change from one boundary condition to another, i.e., at the interfaces between the noflow boundary segment Γ_{else} and the remaining parts Γ_{in} and Γ_{out}. The final grid used for computations is then generated by local refinement of each patch of the superelement grid.

When viewed locally on a given element, the bilinear approximation of p makes each component of the Darcy velocity $\mathbf{v}$ linear in one spatial variable and constant in the other. Since the input data in (1.1), including the mobility tensor Λ, are assumed to be constant on each element, the norms $\|p_1 - p_2\|_{H^1(\Omega)}$ and $\|\mathbf{v}_1 - \mathbf{v}_2\|_{(L^2(\Omega))^2}$ in Corollary 3.1 can be computed analytically. Naturally, this is also possible for the $\|\Lambda^{(1)} - \Lambda^{(2)}\|_{L^\infty(\Omega)}$ norm used in §3 to measure mobility perturbations.

Both for the conforming and the mixed method we have solved the problems on a series of grids with decreasing mesh size. The results reported below correspond to the finest grid for each case, where the computed stability measures seem to be reasonable estimates for the nondiscretized problem.

All computations have been carried out in double precision on HP 9000/735 workstations. The implementations are based on the C++ class library Diffpack, which is under development at SINTEF and the University of Oslo, see Langtangen [13] and [**?**].

4.1. Case I: A simple test problem. In Corollary 3.1, we have established the existence of positive constants c_1 and c_2 independent of the mesh size h, such that

$$\begin{aligned} \frac{\|p_1 - p_2\|_{H^1(\Omega)}}{\|\Lambda^{(1)} - \Lambda^{(2)}\|_{L^\infty(\Omega)}} &\leq c_1, \\ \frac{\|\mathbf{v}_1 - \mathbf{v}_2\|_{(L^2(\Omega))^2}}{\|\Lambda^{(1)} - \Lambda^{(2)}\|_{L^\infty(\Omega)}} &\leq c_2. \end{aligned} \tag{4.1}$$

As in §3, p_1 and p_2 denote the weak solutions of the model problem corresponding to the mobility tensors $\Lambda^{(1)}$ and $\Lambda^{(2)}$, respectively. In order to investigate these estimates experimentally, let us focus on the following problem: Let $\Omega = [0,1]^2$ be divided into three disjoint subdomains

$$\begin{aligned} \Omega_1 &= [0.1, 1] \times [0.2, 0.4], \\ \Omega_2 &= [0, 0.7] \times [0.6, 0.8] \\ \text{and } \Omega_3 &= \Omega \setminus (\Omega_1 \cup \Omega_2), \end{aligned}$$

for which we define the mobility tensor

$$\Lambda^{(1)} = \begin{cases} \begin{bmatrix} 10^{-8} & 0 \\ 0 & 10^{-8} \end{bmatrix} & \text{in } \Omega_1 \cup \Omega_2, \\ \begin{bmatrix} 1 & 0 \\ 0 & 1 \end{bmatrix} & \text{in } \Omega_3. \end{cases}$$

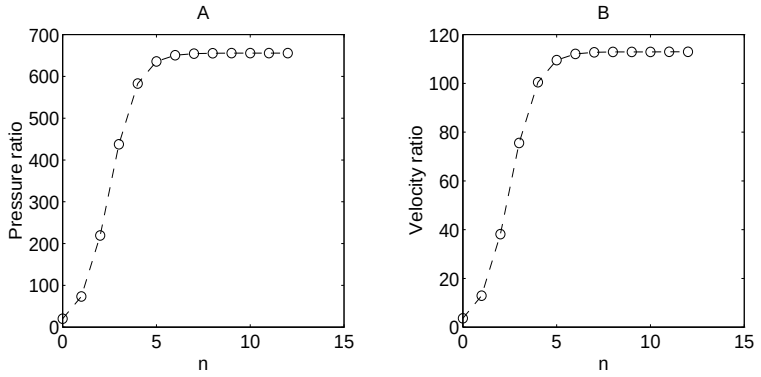

FIG. 1. *The ratios* $\|p_1 - p_{2,n}\|_{H^1(\Omega)} \,/\|\Lambda^{(1)} - \Lambda_n^{(2)}\|_{L^\infty(\Omega)}$ *and* $\|\mathbf{v}_1 - \mathbf{v}_{2,n}\|_{(L^2(\Omega))^2} \,/\|\Lambda^{(1)} - \Lambda_n^{(2)}\|_{L^\infty(\Omega)}$ *as functions of* n *for case I.*

Moreover, the sequence $\{\Lambda_n^{(2)}\}$ is given by

$$\Lambda_n^{(2)} = \begin{cases} \Lambda^{(1)} + \delta_n \begin{bmatrix} 1 & 0 \\ 0 & 1 \end{bmatrix} & \text{in } \Omega_1 \cup \Omega_2, \\ \Lambda^{(1)} & \text{in } \Omega_3, \end{cases}$$

where $\delta_n = 2^{-2n}$ for $n = 0, 1, \ldots, 12$. Consequently, $\Lambda_n^{(2)}$ will quickly approach the fixed tensor $\Lambda^{(1)}$ as n increases, and $\Lambda^{(1)}, \Lambda_n^{(2)} \in A_{10^{-8},1+10^{-8}}$ for all values of n. The boundary conditions on

$$\begin{aligned} \Gamma_{\text{in}} &= \{(x_1, x_2);\ x_1 = 0 \text{ and } x_2 \in [0.9, 1]\}, \\ \text{and} \quad \Gamma_{\text{out}} &= \{(x_1, x_2);\ x_1 = 1 \text{ and } x_2 \in [0, 0.1]\} \end{aligned}$$

are given by $g_{\text{in}} = -10$ and $p_{\text{out}} = 10$. The effect of gravity is neglected.

Figure 1 shows the behaviour of the two ratios in (4.1) as functions of n. For the solutions computed by the conforming finite element method with global mesh size $h = 0.025$, it seems clear that the constants in (4.1) are at least $c_1 \approx 655.7$ and $c_2 \approx 113.0$. For all $n \geq 7$, the computed ratios are close to these bounds.

4.2. Case II: A vertical reservoir section. As for the previous case, we will investigate the effect of mobility values varying on a fixed geometry. In order to relate the stability analysis to reservoir simulation, we consider $\Omega = [0, 1000] \times [0, 20]$ as a vertical section of a reservoir. This domain is divided into different layers

$$\begin{aligned} \Omega_1 &= [0, 300] \times [0, 4] \ \cup \ [400, 1000] \times [0, 4], \\ \Omega_2 &= [0, 700] \times [8, 14] \ \cup \ [800, 1000] \times [8, 14] \\ \text{and} \quad \Omega_3 &= \Omega \setminus (\Omega_1 \cup \Omega_2), \end{aligned}$$

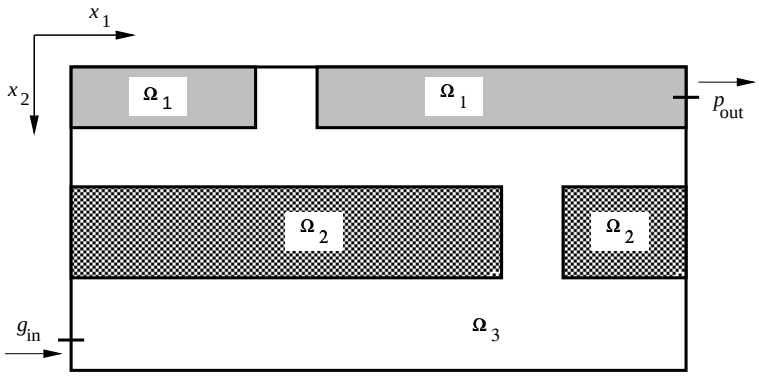

FIG. 2. *The structure of the reservoir used in case II.*

see Figure 2. We assume that the x_2-axis points in the direction of gravity, i.e., we have $\nabla D = (0,1)^T$, while $\rho = 1$ and $g = 9.81$. The boundary conditions are fully specified by (1.2), where

$$g_{\text{in}} = -10 \quad \text{on} \quad \Gamma_{\text{in}} = \{(x_1, x_2);\ x_1 = 0 \text{ and } x_2 \in [18, 20]\} \tag{4.2}$$

and

$$p_{\text{out}} = 1000 \quad \text{on} \quad \Gamma_{\text{out}} = \{(x_1, x_2);\ x_1 = 1000 \text{ and } x_2 \in [0, 2]\}\,. \tag{4.3}$$

In this experiment, we compute p_1 and $\mathbf{v}_1$ for the fixed mobility tensor

$$\Lambda^{(1)} = \begin{cases} \begin{bmatrix} 2 & 0 \\ 0 & 10^{-4} \end{bmatrix} & \text{in } \Omega_1, \\ \begin{bmatrix} 10^{-4} & 10^{-8} \\ 10^{-8} & 10^{-4} \end{bmatrix} & \text{in } \Omega_2, \\ \begin{bmatrix} 2 & 1 \\ 1 & 2 \end{bmatrix} & \text{in } \Omega_3. \end{cases}$$

That is, the layers Ω_1 and Ω_2 are low-permeable in one or both directions. Next we define the sequence $\{\Lambda_n^{(2)}\}$ by

$$\Lambda_n^{(2)} = \begin{cases} \Lambda^{(1)} + \delta_n \begin{bmatrix} 1 & 0 \\ 0 & 1 \end{bmatrix} & \text{in } \Omega_1 \cup \Omega_2, \\ \Lambda^{(1)} & \text{in } \Omega_3, \end{cases}$$

for $\delta_n = 2^{-n}$, $n = 0, 1, \ldots, 19$. Thus, we have $\Lambda^{(1)}, \Lambda_n^{(2)} \in A_{10^{-4}-10^{-8},3}$ for all values of n .

Figure 3 shows the values of the ratios defined in (4.1) obtained for the present problem. These results were computed on a grid with the largest element of size 25×0.5. The behaviour is quite different from the previous case, where the upper bounds c_1 and c_2 seemed to be sharp for large n. However, for the present case, the graphs in Figure 3 reach their maximum for $n = 15$, just before

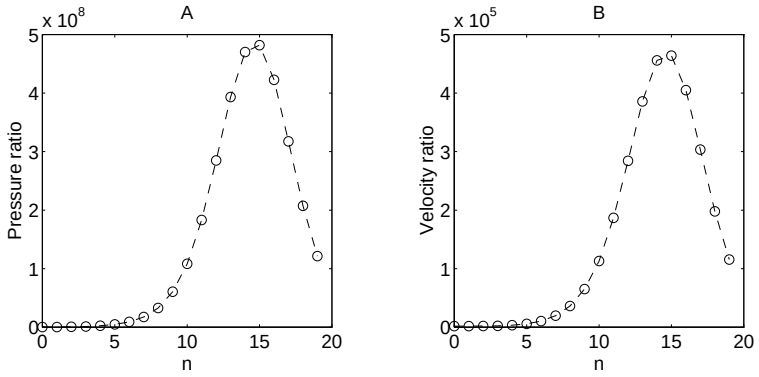

FIG. 3. *The ratios* $\|p_1 - p_{2,n}\|_{H^1(\Omega)} \,/\|\Lambda^{(1)} - \Lambda_n^{(2)}\|_{L^\infty(\Omega)}$ *and* $\|\mathbf{v}_1 - \mathbf{v}_{2,n}\|_{(L^2(\Omega))^2} \,/\|\Lambda^{(1)} - \Lambda_n^{(2)}\|_{L^\infty(\Omega)}$ *as functions of* n *for case II.*

they start to decrease monotonously. This indicates that the stability estimates in Corollary 3.1 hold with $c_1 \approx 4.82 \cdot 10^8$ and $c_2 \approx 4.65 \cdot 10^5$. That is, this particular problem is less sensitive to mobility perturbations than what is predicted by the theory in §3. Given the relatively high complexity of the present example, this observation is somewhat surprising.

4.3. Mixed finite element computations. As mentioned at the beginning of this section, the two cases described in §4.1 and §4.2 have been solved also by a mixed finite element method. In this way, we have a reasonable possibility to verify the results obtained with conforming elements.

Although there is a considerable interest in the use of mixed methods for problems in reservoir simulation (see for example Douglas et al. [6] and Ewing and Wheeler [8]), it is in general not clear whether such methods are preferable to conforming procedures. Falk and Osborne [9] have recently showed that the mixed approach may be less accurate than conforming methods when applied to two-dimensional second-order elliptic problems with rough coefficients.

Before discussing the actual computations, we outline the mixed formulation of our model problem. The pressure equation (1.1) may be stated as a system of two first order equations

$$\begin{aligned} \nabla \cdot \mathbf{v} &= \frac{q}{\rho}, \\ \Lambda^{-1}\mathbf{v} + \nabla p &= \rho g \nabla D \end{aligned} \tag{4.4}$$

in Ω, subject to the boundary conditions (1.2). As before, the entities Λ and $\mathbf{v}$ denote the mobility tensor and the velocity vector, respectively. To derive a weak form of this mixed problem, we introduce the spaces

$$H(\mathrm{div};\Omega) = \left\{\boldsymbol{\psi} \in (L^2(\Omega))^2;\ \nabla \cdot \boldsymbol{\psi} \in L^2(\Omega)\right\}$$

and

$$H_0(\mathrm{div};\Omega) = \left\{\boldsymbol{\psi} \in H(\mathrm{div};\Omega);\ \boldsymbol{\psi} \cdot \mathbf{n} = 0 \text{ on } \Gamma_{\mathrm{in}} \cup \Gamma_{\mathrm{else}}\right\}.$$

Using the test functions $\phi \in L^2(\Omega)$ and $\boldsymbol{\psi} \in H_0(\mathrm{div};\Omega)$, we obtain the standard mixed formulation of the system (4.4):

Find $(p, \mathbf{v}) \in L^2(\Omega) \times \widetilde{H}(\mathrm{div};\Omega)$ such that

$$
\begin{aligned}
a(\mathbf{v},\boldsymbol{\psi}) + b(\boldsymbol{\psi},p) &= G(\boldsymbol{\psi}) \qquad \forall \boldsymbol{\psi} \in H_0(\mathrm{div};\Omega), \\
b(\mathbf{v},\phi) &= F(\phi) \qquad \forall \phi \in L^2(\Omega).
\end{aligned} \tag{4.5}
$$

Here

$$
\widetilde{H}(\mathrm{div};\Omega) = \{\boldsymbol{\psi} \in H(\mathrm{div};\Omega);\ \boldsymbol{\psi}\cdot\mathbf{n} = g_{\mathrm{in}} \text{ on } \Gamma_{\mathrm{in}} \text{ and } \boldsymbol{\psi}\cdot\mathbf{n} = 0 \text{ on } \Gamma_{\mathrm{else}}\},
$$

while the bilinear forms are defined as

$$
a(\mathbf{v},\boldsymbol{\psi}) = \int_\Omega (\Lambda^{-1}\mathbf{v})\cdot\boldsymbol{\psi}\,dx \quad \text{and} \quad b(\boldsymbol{\psi},p) = -\int_\Omega (\nabla\cdot\boldsymbol{\psi})\,p\,dx.
$$

Finally, the linear functionals on the right hand side of (4.5) are given by

$$
F(\phi) = -\int_\Omega \frac{q}{\rho}\phi\,dx \quad \text{and} \quad G(\boldsymbol{\psi}) = \int_\Omega \rho g \nabla D\cdot\boldsymbol{\psi}\,dx - \int_{\Gamma_{\mathrm{out}}} p_{\mathrm{out}}\,(\boldsymbol{\psi}\cdot\mathbf{n})\,ds.
$$

When applying the mixed method to the test problems, we have used the same grid partitionings as for the conforming method. However, in the mixed case we approximate the pressure p as a piecewise constant function evaluated in the center of each element, while the velocity $\mathbf{v}$ is determined by the values of $\mathbf{v}\cdot\mathbf{n}$ in the midpoints of each element side. As for the conforming method, each component of $\mathbf{v}$ is linear in one spatial variable and constant in the other when viewed locally on a particular element. Thus, the norms involved in the stability analysis can still be computed by exact integration.

The described mixed elements, which are often referred to as the lowest order Raviart-Thomas elements (cf. [16]), correspond to a certain choice of finite-dimensional subspaces $W \subset \widetilde{H}(\mathrm{div};\Omega)$ and $Q \subset L^2(\Omega)$. These subspaces are known to be balanced in the sense that they fulfill the inf-sup condition, i.e., there exists a constant η independent of the mesh size h such that

$$
\inf_{\phi\in Q}\sup_{\boldsymbol{\psi}\in W} \frac{b(\boldsymbol{\psi},\phi)}{\|\phi\|_{L^2(\Omega)}\|\boldsymbol{\psi}\|_{\mathrm{div},\Omega}} \geq \eta > 0. \tag{4.6}
$$

Roughly speaking, this condition says that the velocity space must be chosen large enough for a given pressure space. Moreover, these subspaces also satisfy

$$
\sup_{\phi\in Q} b(\boldsymbol{\psi},\phi) > 0
$$

for all $\boldsymbol{\psi} \in W$ such that $\nabla\cdot\boldsymbol{\psi} \neq 0$. Together with (4.6) this inequality ensures numerical stability of the method, cf. [1, 16]. For further details on alternative choices of mixed elements and their corresponding subspaces, we refer to [2, 3, 16].

Let us now turn to the results obtained for the problems in §4.1 and §4.2. For the first case we have compared the results produced by the two solution procedures using a grid with maximum mesh

size $h = 0.05$. The ratios in (4.1) shows the same qualitative behaviour for the mixed method as previously reported for the conforming solver, i.e., they are close to their respective upper bounds for $n \geq 7$. However, the pressure ratio computed by the mixed method takes on much smaller values. In fact, the estimated bound is then $c_1 \approx 198.8$, opposed to the value $c_1 \approx 630.9$ obtained for the conforming method, see Figure 4. Presumably, this difference is due to incomparable representations of the pressure solution. In the mixed case p is piecewise constant, thus neglecting the possibly large values of ∇p when computing the H^1 norm of the change of the pressure. This explanation is supported by the comparison of computed velocities. Both methods represent the velocity by components that are piecewise linear in one spatial variable and piecewise constant in the other[1]. This leads to the estimated bounds $c_2 \approx 114.6$ and $c_2 \approx 113.1$ for the mixed and conforming methods, respectively.

Turning to the second test problem, the computations have been performed for a grid with the largest element of size 50×1. In contrast to the first case, the two methods produce almost identical results even for the pressure ratio. For both norms, the curves reach their maximum value for $n = 15$ before they start to decrease monotonously, see Figure 5.

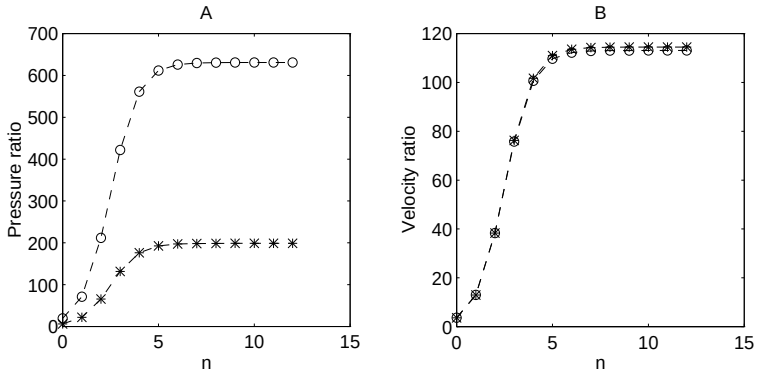

FIG. 4. *The ratios* $\|p_1 - p_{2,n}\|_{H^1(\Omega)} / \|\Lambda^{(1)} - \Lambda_n^{(2)}\|_{L^\infty(\Omega)}$ *and* $\|\mathbf{v}_1 - \mathbf{v}_{2,n}\|_{(L^2(\Omega))^2} / \|\Lambda^{(1)} - \Lambda_n^{(2)}\|_{L^\infty(\Omega)}$ *as a function of* n *for case III. The symbols* $\circ$ *and* $*$ *denote the conforming and the mixed finite element solutions, respectively.*

5. Concluding remarks. We have investigated the effect of mobility perturbations on the pressure and velocity obtained for a typical two-dimensional pressure equation. Analytical estimates have been derived that bound the changes in the pressure and velocity in terms of mobility perturbations measured by the L^∞ norm.

Through a series of numerical experiments that allow the mobility to change in value we have complemented the stability analysis. We have also observed that there are problems where the actual

[1] Based on these observations, one might argue that higher order mixed elements should be used in order to obtain representative estimates for $\|p_1 - p_{2,n}\|_{H^1(\Omega)}$. However, in the context of reservoir simulation the vital entity is the velocity $\mathbf{v}$, which is used as input to other equations in the overall simulation process. We also note that the pressure ratio obtained when applying the mixed solver to the second test problem are close to the values computed by the conforming method.

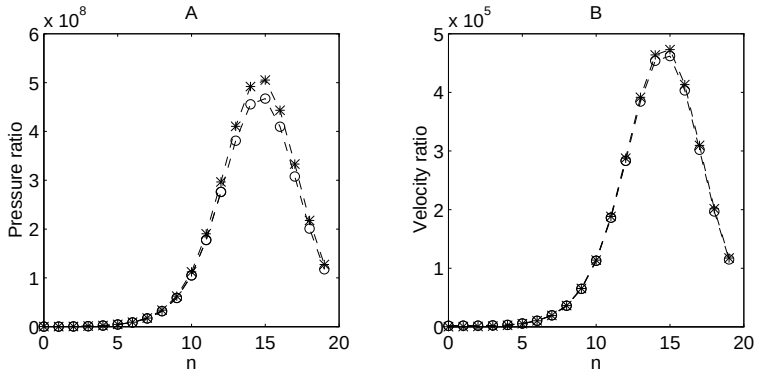

FIG. 5. *The ratios* $\|p_1 - p_{2,n}\|_{H^1(\Omega)} / \|\Lambda^{(1)} - \Lambda_n^{(2)}\|_{L^\infty(\Omega)}$ *and* $\|\mathbf{v}_1 - \mathbf{v}_{2,n}\|_{(L^2(\Omega))^2} / \|\Lambda^{(1)} - \Lambda_n^{(2)}\|_{L^\infty(\Omega)}$ *as a function of* n *for case III. The symbols* $\circ$ *and* $*$ *denote the conforming and the mixed finite element solutions, respectively.*

behaviour is less sensitive to mobility perturbations than what is indicated by the theory.

The numerical results have been verified by independent computations based on both conforming and mixed finite element solutions of the test cases.

Acknowledgements. The authors want to thank the professors Ragnar Winther and Aslak Tveito for valuable discussions and for encouraging the work presented in this paper. We also want to thank Wen Shen for help with the programming of the mixed finite element code. Finally, we want to thank one of the referees for valuable remarks and guidance, improving the readability of the paper.

REFERENCES

[1] F. BREZZI, *On the existence, uniqueness and approximation of saddle-point problems arising from Lagrangian multipliers*, RAIRO Numer. Anal., 8 (1974), pp. 129–151.

[2] F. BREZZI, J. DOUGLAS JR., M. FORTIN, AND L. D. MARINI, *Efficient rectangular mixed finite elements in two and three space variables*, RAIRO Modél. Math. Anal. Numér., 21 (1987), pp. 581–604.

[3] F. BREZZI, J. DOUGLAS JR., AND L. D. MARINI, *Two families of mixed finite elements for second order elliptic problems*, Numer. Math., 47 (1985), pp. 217–235.

[4] R. DAUTRAY AND J.-L. LIONS, *Mathematical Analysis and Numerical Methods for Science and Technology*, vol. II: Functional and Variational Methods, Springer-Verlag, 1988.

[5] ———, *Mathematical Analysis and Numerical Methods for Science and Technology*, vol. I, Physical Origins and Potential Theory, Springer-Verlag, 1990.

[6] J. DOUGLAS JR., R. E. EWING, AND M. F. WHEELER, *The approximation of the pressure by a mixed method in the simulation of miscible displacement*, R. A. I. R. O. Numer. Anal., 17 (1983), pp. 17–33.

[7] R. E. EWING, *Problems arising in the modeling of processes for hydrocarbon recovery*, in Compressible Fluid Flow and Systems of Conservation Laws in Several Space Dimensions, A. Majda, ed., Springer-Verlag, 1984, pp. 3–34.

[8] R. E. EWING AND M. F. WHEELER, *Computational aspects of mixed finite element methods*, in Scientific Computing, R. Stepleman, M. Carver, R. Peskin, W. F. Ames, and R. Vichnevetsky, eds., vol. I of IMACS Transactions on Scientific Computation, North-Holland, 1983, pp. 163–172.

[9] R. S. Falk and J. E. Osborn, *Remarks on mixed finite element methods for problems with rough coefficients*, Math. Comp., 62 (1994), pp. 1–19.

[10] G. B. Folland, *Real Analysis. Modern Techniques and Their Applications*, John Wiley & Sons, 1984.

[11] D. Gilbarg and N. S. Trudinger, *Elliptic Partial Differential Equations of Second Order*, Springer-Verlag, 1977.

[12] W. Hackbusch, *Elliptic Differential Equations. Theory and Numerical Treatment*, Springer-Verlag, 1992.

[13] H. P. Langtangen, *Diffpack: Software for partial differential equations.* (To appear in the proceedings of the 2nd Annual Object-Oriented Numerics Conference, Sunriver, Oregon), 1994.

[14] J. A. Meijerink and H. A. van der Vorst, *An iterative solution method for linear systems of which the coefficient matrix is a symmetric M-matrix*, Math. Comp., 31 (1977), pp. 148–162.

[15] D. W. Peaceman, *Fundamentals of Numerical Reservoir Simulation*, Elsevier, 1977.

[16] P. A. Raviart and J. M. Thomas, *A mixed finite element method for 2-nd order elliptic problems*, in Mathematical Aspects of Finite Element Methods, I. Galligani and E. Magenes, eds., vol. 606 of Lect. Notes in Math., Springer-Verlag, 1977, pp. 292–315.